

OBJECTIVES

The aim of this work is to assess the impact of data assimilation on the dynamics of mesoscale eddies. We do this based on the use of a recent mathematical method from nonlinear dynamics field that is capable of detecting Lagrangian eddies from birth to death. We apply this method on two composites time series of two configurations covering the whole globe, with and without assimilation, and carry on various statistical analysis to evaluate the impact of data assimilation on several properties of these Lagrangian mesoscale eddies.

MATERIALS & METHODS

1 DATA

Two sets of velocity field covering three different periods of time are used in this study, presenting the first level of oceanic current of an oceanic model with and without assimilation. The first set consists of the Ocean ReAnalysis System 5 (ORAS5) products, developed at ECMWF based on NEMO at 1/4° resolution and NEMOVAR-3DFGAT scheme, while the second one (gf8l) represents the same configuration, but without assimilation procedure.

2 Eddy detection method

The method we use here relies on the analysis of the Lagrangian geometrical properties of velocity fields and the use of a grid density-based clustering algorithm [1]. The method can be summarized in the three following steps:

- (i) It starts by segmenting Lagrangian trajectories into rotational ($s(t_\beta, t_\alpha, \mathbf{x}_0)$, with $sgn(\theta(t_\beta, t_\alpha, \mathbf{x}_0))$ such that $\forall \theta(t) \in \theta(t_\beta, t_\alpha, \mathbf{x}_0), \theta(t) > 0$ or $\forall \theta(t) \in \theta(t_\beta, t_\alpha, \mathbf{x}_0), \theta(t) < 0$) and non-rotational segments based on the geometrical properties of their evolving velocities.

$$\theta(t_{i+1}, t_i, \mathbf{x}_0) = \cos^{-1} \frac{\vec{v}(\mathbf{x}_0, t_i) \cdot \vec{v}(\mathbf{x}_0, t_{i+1})}{|\vec{v}(\mathbf{x}_0, t_i)| |\vec{v}(\mathbf{x}_0, t_{i+1})|}, i \in [\alpha, \beta[\quad (1)$$

- (ii) It maps the initial and final position of the extracted rotational segments.

$$\{\mathbf{x}_i(t_{i_\alpha}), \mathbf{x}_i(t_{i_\beta})\}_{i=0}^n = \left\{ \Phi_{t_0}^{t_{i_\alpha}}(\mathbf{x}_i(t_0)), \Phi_{t_0}^{t_{i_\beta}}(\mathbf{x}_i(t_0)) \right\}_{i=0}^n, \quad (2)$$

$$\{t_{i_\alpha}\}_{i=0}^n \in [t_0, t_f[, \quad \{t_{i_\beta}\}_{i=0}^n \in]t_0, t_f]$$

- (iii) It uses a grid density-based clustering algorithm to group them into different classes characterized by different transport properties, which represent the coherent cores of the eddies.

$$N_{j \in \alpha}(\{\mathbf{x}_i(t_{i_\alpha})\}_{i=1}^n, p_j) = \{p_j, p_k \in \{\mathbf{x}_i(t_{i_\alpha})\}_{i=1}^n : d(p_j, p_k) \leq \epsilon\} \quad (3)$$

$$N_{j \in \beta}(\{\mathbf{x}_i(t_{i_\beta})\}_{i=1}^n, p_j) = \{p_j, p_k \in \{\mathbf{x}_i(t_{i_\beta})\}_{i=1}^n : d(p_j, p_k) \leq \epsilon\}$$

where $N_{j \in \alpha}$ is a function that associates to each particle p_j a given density based on its neighboring. $d(p_j, p_k)$ denotes the Euclidean distance between particle p_j and p_k . ϵ is the minimum Euclidean distance for neighboring. We define a coherent eddy as a time-evolving domain:

$$\mathbf{E} = \bigcup_{t \in [t_\alpha, t_\beta]} \mathbf{E}(t) \subset \mathbb{R}^2 \times [t_\alpha, t_\beta], \quad (4)$$

in a way that \mathbf{E} is a set of adjacent particles $\{\mathbf{x}_j\}_{j=0}^m$ characterized by rotational segments that co-exist in the dense regions $G(t_\alpha) = \{N_{j \in \alpha}\}_{j=0}^m$ and $G(t_\beta) = \{N_{j \in \beta}\}_{j=0}^m$ respectively at t_α and t_β :

$$\mathbf{E} = G(t_\alpha) \cap G(t_\beta) \quad (5)$$

REFERENCES

- [1] Anass El Aouni. A hybrid identification and tracking of lagrangian mesoscale eddies. *Physics of Fluids*, 33(3):036604, 2021.

RESULTS 2

Figure.1 shows the statistical distribution of the genesis of Lagrangian eddies in both datasets and over different period of time, highlighting both variation of eddies activity both between period of times and between configurations.

Figure.3 shows Hovmoller diagrams at 1°/30-day spatio-temporal resolution of the eddies intensity, where the main patterns can be synthesized into regions of permanent and seasonal eddies activities.

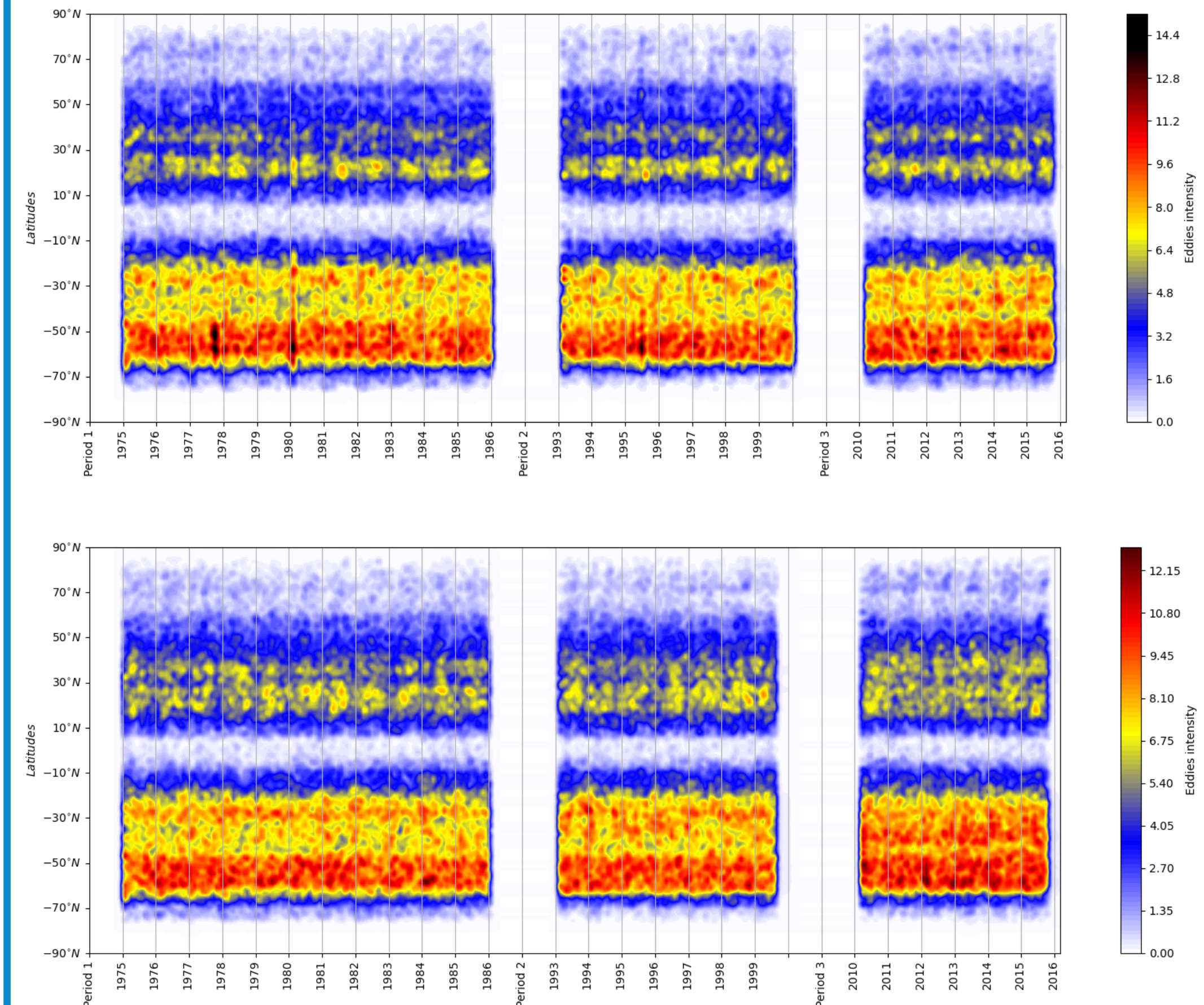


Figure 3: A hovmoller plot displaying meridional-temporal variation of eddies activity in gf8l (upper panel) and oras5 (bottom).

Figure.2 shows both the monthly variation of the number of eddies in both configurations and over three different periods of time, characterized by a considerable year-to-year variability and oscillations between periods strong and weaker eddies intensities, with clear anomalies such as 1977, 1980 and 1995. In the same Figure, we show the meridional climatology of the eddies activity, in which we clearly observe the impact of the assimilation on the eddies dynamics.

	<R>		<L>		<Td>	
Period	gf8l	oras5	gf8l	oras5	gf8l	oras5
1975~1985	78	79	123	121	191	194
1993~1999	79	80	120	117	200	200
2010~2015	79	79	121	114	197	201

Table 1: Physical properties of Lagrangian eddies: (Td(km): traveled distance; L(day): lifetime; R(km): diameter

	Transport (Sv)	
Period	gf8l	oras5
1975~1985	54.22	57.57
1993~1999	54.55	57.42
2010~2015	52.90	60.59

Table 2: Climatology of coherent water transport (Sv) achieved by Lagrangian eddies

RESULTS 1

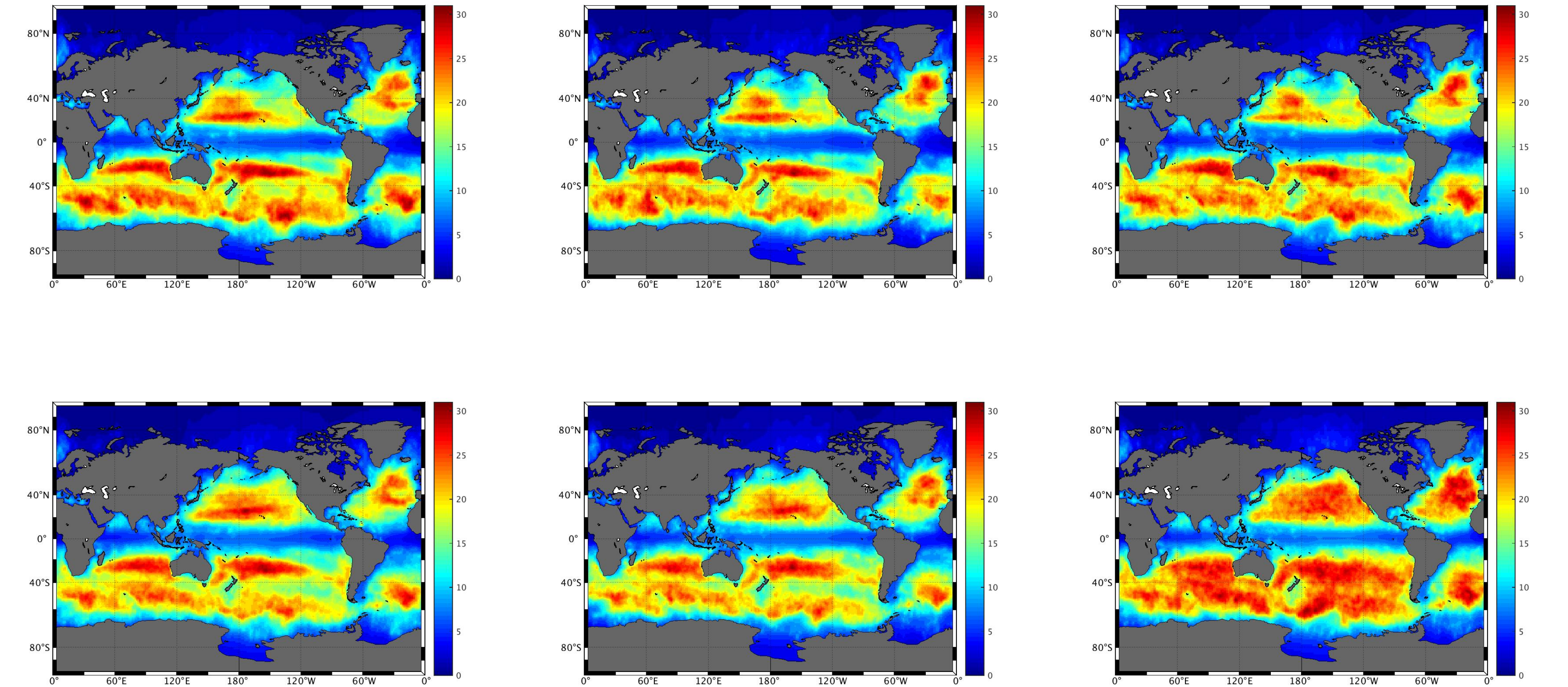


Figure 1: Density distribution of Lagrangian mesoscale eddies here they gain their coherency and form solid cores: gf8l (upper), ORAS5 (bottom), from left to right: 1975~1985, 1993~1999, 2010~2015.

RESULT 3

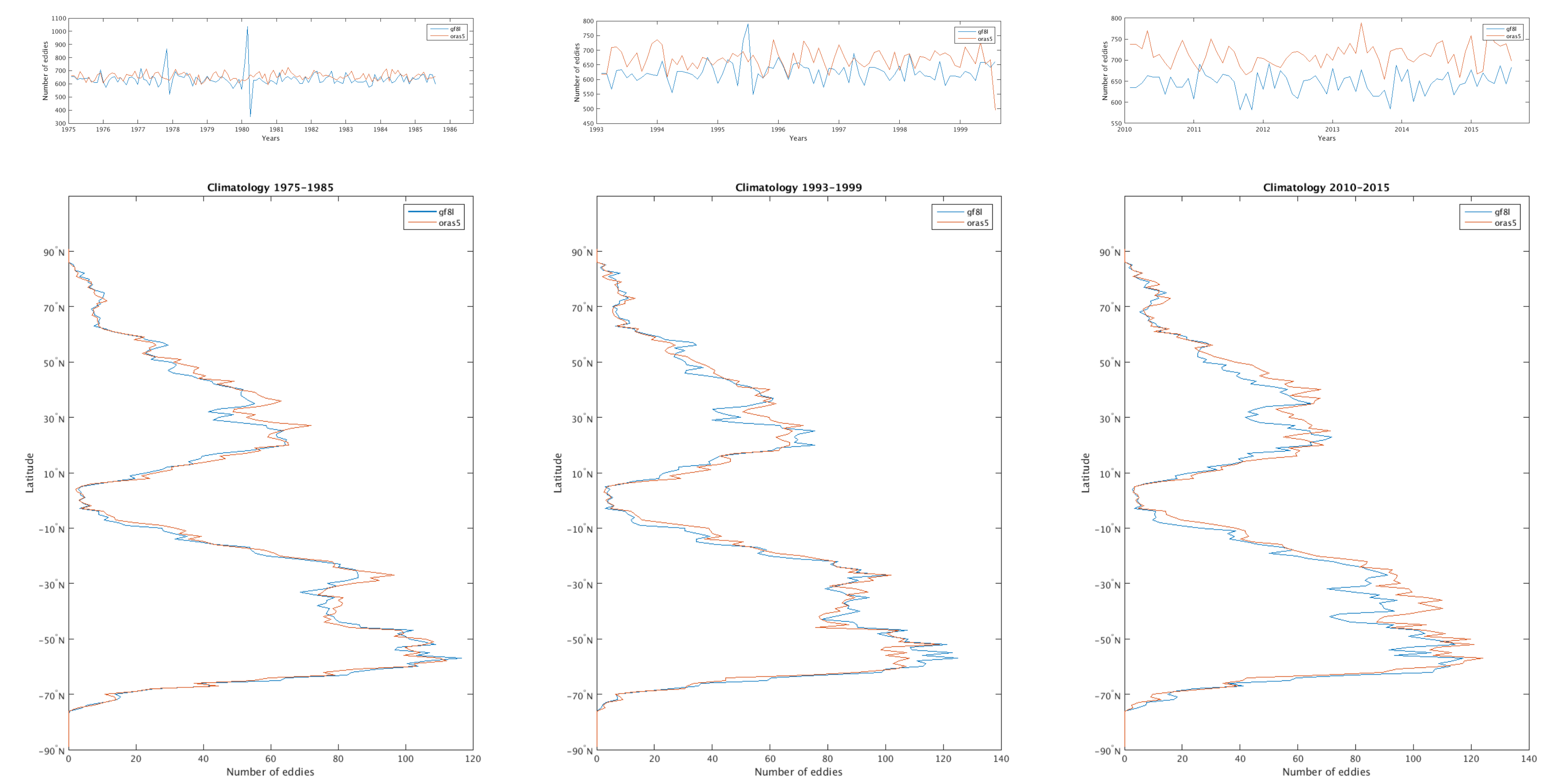


Figure 2: (Upper panel) monthly eddies activity in oras5 and gf8l. (Upper panel) Meridional climatology of the eddies activity for the three periods of time.

SUMMARY

In the light of evaluating the impact of data assimilation procedure on eddies activity, we made use of a recent method from nonlinear dynamics field, together with two historical time series of ocean current derived from ocean model with and without assimilation, then carried on several statistical analysis of various physical properties of Lagrangian eddies over the globe.